Graphical Abstract

A comparison of analytical methods to predict the bulk temperature in polymer spur gears

Victor Roda-Casanova, Carlos M.C.G. Fernandes

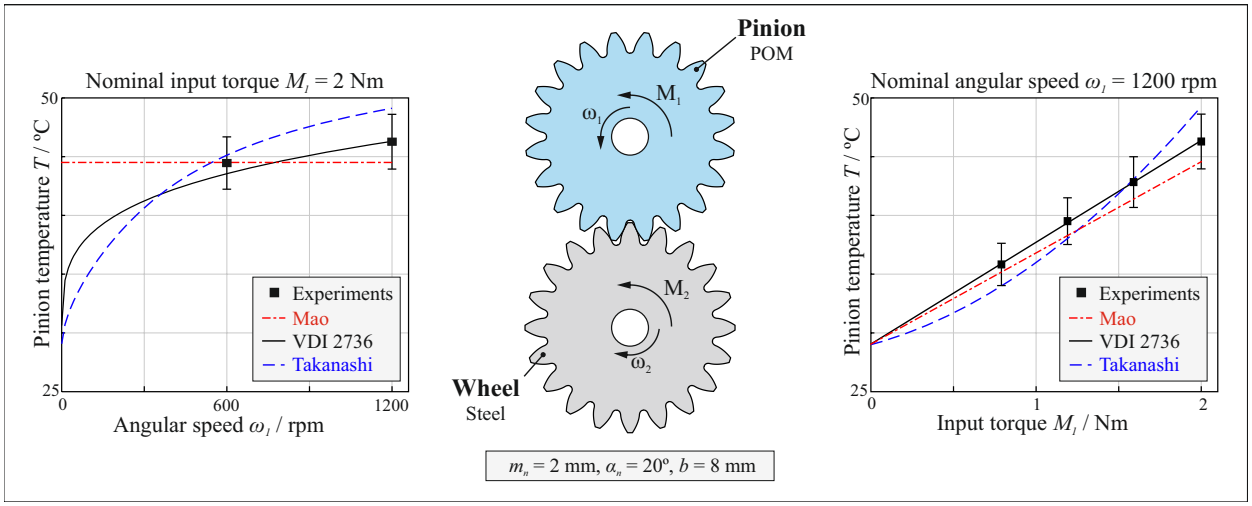

Highlights

A comparison of analytical methods to predict the bulk temperature in polymer spur gears

Victor Roda-Casanova, Carlos M.C.G. Fernandes

- Review of theoretical models that rule the temperature rise phenomena of polymer gears
- Hachmann, Takanashi and Mao methods are explained
- The common points, strengths and limitations of these methods are identified
- The methods are compared to reference experimental results

A comparison of analytical methods to predict the bulk temperature in polymer spur gears

Victor Roda-Casanova[a], Carlos M.C.G. Fernandes[b,*]

[a] *Universitat Jaume I, Av. Sos Baynat s/n, Castello de la Plana, 12071, Spain*
[b] *FEUP, Rua Dr. Roberto Frias s/n, Porto, 4200-465, Portugal*

Abstract

The mechanical properties of polymer gear transmissions are dependent on the operating temperature. Therefore, the prediction of the temperature of polymer gears is an important step during the design process. In this regard, analytical methods provide simple equations to predict the bulk temperature, but its applicability is limited by the underlying theory.

In this work, a detailed background of the theoretical models that affect the temperature rise phenomena of polymer gears is provided. The methods suggested by Hachmann (and its implementation on VDI 2736 standard), Takanashi and Mao are derived from this common theoretical background. The common points, strengths and limitations of the methods are provided.

The methods are illustrated with a variety of numerical examples and compared to reference experimental results. This comparison allowed us to draw some conclusions, to provide recommendations for the application of these methods, and identify potential measures of improving their results.

Keywords: bulk temperature, polymer gear, friction, hysteresis, heat transfer

1. Introduction

Polymer gears are replacing metallic gears in a wide range of applications, as they offer some interesting advantages compared to their metallic counterparts. From the manufacturing point of view, they are easier to manufacture and they have a lower cost than metallic gears, particularly for injection-molded gears. From the operating point of view, polymer gears have a lower mass and a lower inertia than metallic gears, which combined with their capability to dampen shocks and impacts can be advantageous in terms of the dynamic response of the gear unit. Moreover, polymers offer good resistance to corrosion and they have a low dry contact coefficient of friction, which enables polymer gear transmissions to operate without lubricant.

*Corresponding author
Email address: cfernandes@fe.up.pt (Carlos M.C.G. Fernandes)

Compared to metallic gears, the applicability of polymer gears is mainly limited by their low load carrying capacity and their sensitivity to the changes in their operating temperature. Increments of temperature diminish the mechanical properties of polymer gear transmissions: they reduce the elastic modulus of the polymer gear material, as well as the bending and the rolling contact fatigue strength of the gears [1]. This is especially problematic, since geared transmissions are subjected to elevated temperature increments produced by the combined effect of a significant heat generation during the meshing of the teeth and a low heat dissipation. For these reasons, the prediction of the temperature of the gears in operating conditions is an important step during the design process of polymer gear transmissions.

The determination of the operating temperature of polymer gears can either be accomplished by numerical or analytical methods. In the great majority of these methods, the temperature rise of the gears is described by the superposition of two contributions: the bulk and the flash temperatures [2]. The bulk temperature denotes the long-term temperature rise throughout the gear structure. The flash temperature defines the local, almost instantaneous, temperature rise around the heat source [3, 4]. Both temperature contributions can have important consequences over the integrity of polymer gears: the increment of the bulk temperature reduces the fatigue strength of the gears [1, 5] and can cause the yielding of the polymer material [6], whereas the flash temperature is related to the scuffing of the gear surfaces [7].

Although some exceptions can be found [8–10], numerical methods for the determination of the operating temperature of polymer gears are usually based on a finite element thermal analysis. Relevant works in this field are those conducted by Fernandes [11, 12], Roda-Casanova [13–15] and Černe [4]. In general, these numerical methods provide a comprehensive description of the temperature field along the polymer gears in operating conditions, but they usually require elevated preparation times and they have an additional computational cost. A big computational cost can be an important issue, specially when these methods are used for gear optimization purposes [16, 17]. Moreover, they require knowledge and resources that may not always be available to the gear designer.

On the other hand, analytical methods are typically fast and easy to implement. Here, the methods for calculating the flash and the bulk temperature differ. The most important method for the calculation of the flash temperature is provided by Blok [3]. Blok's method has been adopted by several gear design standards to assess metallic gears scuffing, and it has been analysed in depth in the works of Tobe [18] and Mao [19].

Regarding the analytical methods to determine the bulk temperature of polymer gears, the most simple ones are those consisting in empirical equations in which a set of coefficients is adjusted to match the results obtained from experimental analyses. Examples of empirical models were proposed by Gauvin [20] or the one included in ESDU 68001 [21]. These models can be useful in some situations, but their applicability is limited by the number of experiments carried out to tune the adjusting coefficients [19] and they usually bring small physical insight into the problem.

More comprehensive analytical methods to calculate the bulk temperature of polymer gears are based on the first law of thermodynamics. In these methods the bulk temperature

of the gears is calculated by establishing a thermal equilibrium between the heat generated during the meshing of the gears and the thermal energy dissipated by heat transfer mechanisms.

Following this principle, the first relevant method was derived in 1966 by Hachmann and Strickle [22]. In this method, a thermal equilibrium is established between the heat generated by friction and the heat dissipated by convection from the gear. This method has been trusted by important organizations to develop design guidelines and standards such as the VDI 2736 [5] and the BS 6168:1987 [23]. Hachmann's method, or his derived versions, have been widely used in the literature for gear optimization purposes [17, 24], to examine the durability of steel/PEEK gear pairs [25], to investigate the potential of bio-based polymer gears [26], and to compare its results to the ones obtained from experimental analyses [27, 28].

More than a decade later, Takanashi and Shoji [29, 30] proposed a method in which the thermal equilibrium is established between the heat generated by friction/hysteresis and the heat dissipated by convection. The Takanashi method has been subjected to several enhancements, either made by the author himself [31, 32] or by other authors [33], and its performance was validated by Terashima [34]. In detriment of Takanashi's method it must be said that several authors [28, 35] have pointed out that this method is difficult to use because of the lack of material data in the literature to calculate the hysteresis losses.

More recently, an analytical method for the calculation of the bulk temperature of polymer gears was developed by Hooke and Mao [36] in 1993. In this method the thermal behaviour of the gear unit is approached to that one of a gear pump, and the thermal equilibrium is established between the heat generated by friction and the heat dissipated by convection. The method was validated by experimental analyses conducted by Mao, and also by other authors [37].

These analytical methods provide relatively simple equations that allow to predict the bulk temperature of polymer gear transmissions, but its applicability is limited due to its underlying theory. So, in order to obtain reliable results from the application of these methods, it is very important to know and understand these limitations. Thus, in this work, the methods proposed by Hachmann [22], Takanashi [30] and Mao [19] are analysed and compared with the following objectives:

1. To provide a detailed background of the theoretical models that affect the temperature rise phenomena of polymer gears (frictional and hysteretic heat generation and convective heat dissipation).
2. To derive the selected models from this common theoretical background, in order to provide a better understanding of their common points, strengths and limitations.
3. To illustrate the application of these methods with a variety of numerical examples and compare the obtained results to reference experimental results.

2. Statement of the problem

The great majority of the analytical methods used to predict the bulk temperature of polymer gears are based on the first law of thermodynamics. This law establishes that the

net change in the total energy of the system ΔE is equal to the difference between the total energy entering the system E_{in} and the total energy leaving the system E_{out} during that process.

When the first law of thermodynamics is used to predict the bulk temperature of polymer gears, only thermal energy (heat) is taken into account in the energy balance. Furthermore, the bulk temperature is calculated for gears operating in steady state conditions, meaning that there is no energy change in the system (i.e. $\Delta E = 0$). In other words, the heat entering the system must balance the heat leaving the system:

$$E_{in} = E_{out} \tag{1}$$

In polymer gear drives, the heat entering the system comes from two different sources:

- The frictional power losses that are produced as a consequence of the rolling and sliding relative motion between gear teeth. According to tribologists [2], almost all the energy dissipated in frictional contacts is transformed into frictional heat.
- The hysteresis power losses caused by the viscoelastic deformation of the gears, which are mostly dissipated as hysteretic heat. There are several works [4, 38, 39] that report that hysteresis losses are small compared to the frictional losses and, for this reason, they are neglected in some temperature calculation models [5, 19, 22]. In contrast, other works [30] indicate that hysteretic heat may have an important role in the temperature rise of the gears. This controversy indicates that attention must be paid to this phenomenon.

Denoting the heat generated by friction by E_f and the heat generated by hysteresis by E_h, the heat entering the system can be defined as:

$$E_{in} = E_f + E_h \tag{2}$$

On the other hand, heat can be removed from the system by three heat transfer mechanisms [40]:

- Conduction, which is the transfer of energy from the more energetic particles of a substance to the adjacent less energetic ones as a result of interactions between the particles.
- Convection, which is the transfer of energy between a solid surface and the adjacent liquid or gas that is in motion, and it involves the combined effects of conduction and fluid motion.
- Radiation, which is the energy emitted by matter in the form of electromagnetic waves as a result of the changes in the electronic configurations of the atoms or molecules.

In the application of analytical methods to the prediction of the bulk temperature of polymer gears, it is common to consider that the whole thermal system has the same temperature and, in this case, heat conduction vanishes. Moreover, the amount of heat dissipated by radiation is so small compared to the amount of heat dissipated by convection that it is usually neglected in the calculations. Taking this into account, it can be said that all the heat is dissipated from the gears by convection (E_c):

$$E_{out} = E_c \tag{3}$$

Thus, in general and inserting equations (2) and (3) into Eq. (1), the following expression is obtained:

$$E_f + E_h = E_c \tag{4}$$

The previous equation can also be written in terms of average thermal power:

$$\frac{E_f}{t_{cycle}} + \frac{E_h}{t_{cycle}} = \frac{E_c}{t_{cycle}} \rightarrow \hat{Q}_f + \hat{Q}_h = \hat{Q}_c \tag{5}$$

where t_{cycle} is the time it takes to the gear to complete a revolution, $\hat{Q}_f$ is the average frictional power, $\hat{Q}_h$ is the average hysteretic power and $\hat{Q}_c$ is the average convective power. The problem of determining E_f, E_h and E_c (or $\hat{Q}_f$, $\hat{Q}_h$ and $\hat{Q}_c$) is at the core of all the analytical methods used to determine the bulk temperature of polymer gears, and it is covered in the following sections.

3. Heat generated by sliding friction

Consider a spur gear pair as the one shown in Fig. 1a. The pinion is rotating around point O_1 at an angular speed ω_1, and the wheel is rotating around point O_2 at an angular speed ω_2. An input torque M_1 is applied over the pinion, whereas an output torque M_2 is applied at the wheel. The number of teeth of pinion and wheel is given by z_1 and z_2, respectively. Both pinion and wheel have involute profiles, and the contact ratio of the transmission is $1 < \varepsilon_\alpha < 2$.

The point where the pinion profile contacts the gear profile is denoted by point Y. From a theoretical point of view, and since the gears have involute profiles, point Y is always located over a line that is usually referred to as the *line of action*. The line of action is tangent to the pinion and wheel base circles at points N_1 and N_2, respectively. The point where the line of action intersects the line of centers $\overline{O_1O_2}$ is denoted by pitch point C. The position of the point of contact Y with respect to point C is defined by the intrinsic coordinate ξ.

Figure 1b shows some points of interest that can be found over the line of action. Points A and E represent the beginning and the end of the engagement of a pair of teeth, respectively. In the interval comprised between points B and D the contact occurs only between a pair of teeth, whereas outside of the interval BD the contact occurs between two teeth

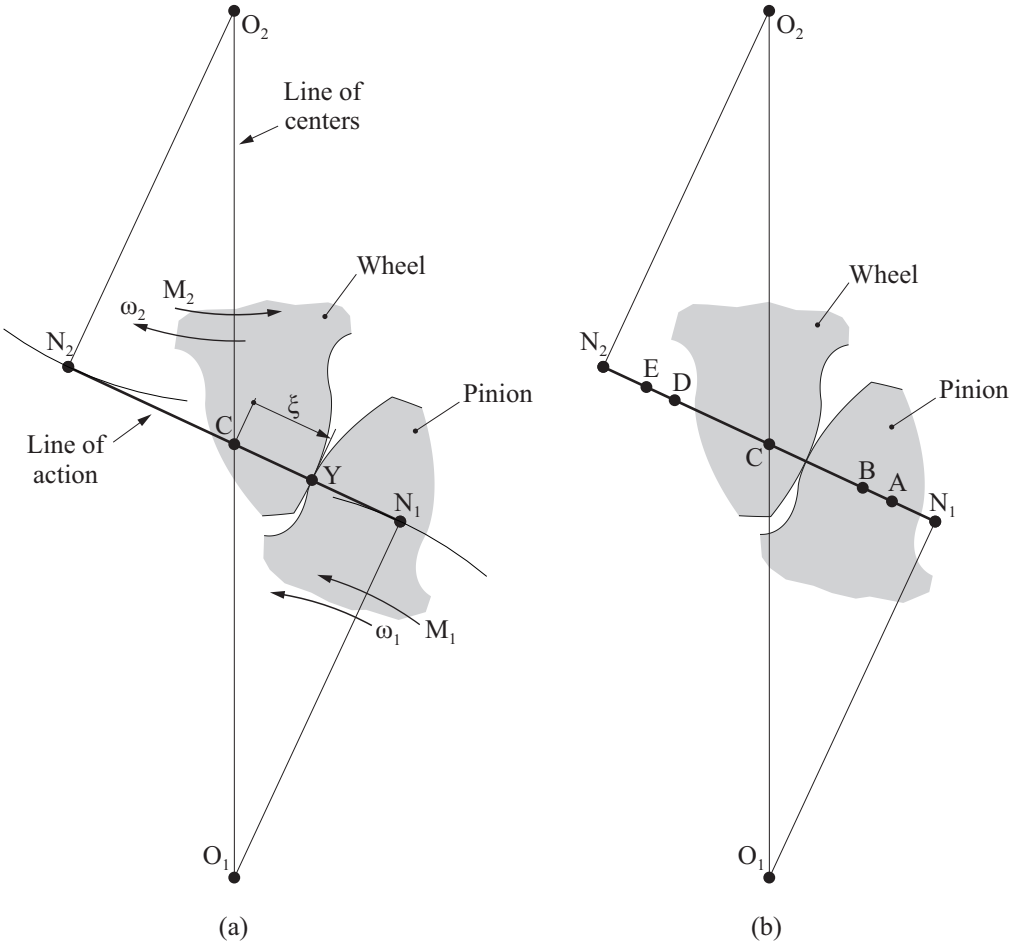

Figure 1: Definition of line of action and points of interest

simultaneously. Each one of these points has an associated intrinsic coordinate ξ_A, ξ_B, ξ_D and ξ_E.

The instantaneous frictional power loss as a consequence of the engagement of a pair of teeth can be defined as:

$$Q_{f,th}(\xi) = F_f(\xi) \cdot v_s(\xi) \tag{6}$$

where $F_f(\xi)$ is the tangential contact force and $v_s(\xi)$ is the sliding speed at the point of contact, which can be calculated as [63]:

$$v_s(\xi) = \left| \omega_1 \cdot \xi \cdot \frac{z_1 + z_2}{z_2} \right| \tag{7}$$

On the other hand, the Coulomb law of friction allows us to relate the tangential contact force $F_f(\xi)$ to the normal contact force $F_n(\xi)$ through the coefficient of friction $\mu(\xi)$. Besides that, it is common to define the normal contact force $F_n(\xi)$ as the multiplication of the nominal load along the line of action F_{bn} by the load sharing function $\beta(\xi)$:

$$F_f(\xi) = \mu(\xi) \cdot F_n(\xi) = \mu(\xi) \cdot F_{bn} \cdot \beta(\xi) \tag{8}$$

Equation (9) may be written by substituting Eq. (8) into Eq. (6), and multiplying and dividing the resulting expression by speed of the point of contact v_{bn}:

$$Q_{f,th}(\xi) = \mu(\xi) \cdot P_{in} \cdot \beta(\xi) \cdot \frac{v_s(\xi)}{v_{bn}} \tag{9}$$

where $P_{in} = F_{bn} \cdot v_{bn}$ is the input power.

Assuming that all the energy dissipated in frictional contacts is transformed into heat, the frictional heat that is generated during the engagement of a pair of teeth can be calculated as:

$$E_{f,th} = \frac{2}{d_{b1} \cdot \omega_1} \int_{\xi_A}^{\xi_E} Q_{f,th}(\xi) \ \mathrm{d}\xi \tag{10}$$

where d_{b1} is the base diameter of the pinion. The average frictional thermal power generated during the meshing of the gears can be calculated as:

$$\hat{Q}_f = \frac{z_1}{t_1} \cdot E_{f,th} = \frac{1}{p_b} \int_{\xi_A}^{\xi_E} Q_{f,th}(\xi) \ \mathrm{d}\xi \tag{11}$$

Here, $t_1 = \frac{2 \cdot \pi \ \mathrm{rad}}{\omega_1}$ is the time it takes to the pinion to complete a revolution and p_b is the base pitch of the transmission.

3.1. Heat partition factor

As stated before, the frictional power losses that occur during the meshing of a pair of teeth are dissipated as frictional heat. Some of this heat goes into the pinion and the rest goes into the wheel, in such a way that the following equation is fulfilled:

$$Q_{f,th}(\xi) = Q_{f,th1}(\xi) + Q_{f,th2}(\xi) \tag{12}$$

where $Q_{f,th1}(\xi)$ is the thermal power entering the pinion tooth and $Q_{f,th2}(\xi)$ is the thermal power entering the wheel tooth. In practice, heat partition is accomplished by means of a heat partition factor $\varphi(\xi)$, which represents the fraction of heat entering the pinion. Thus, the following equation can be written:

$$Q_{f,th1}(\xi) = Q_{f,th}(\xi) \cdot \varphi(\xi) \tag{13}$$

Taking this into account, the frictional heat entering a pinion tooth $E_{f,th1}$ and the average frictional thermal power entering the pinion $\hat{Q}_{f,1}$ can be calculated as:

$$E_{f,th1} = \frac{2}{d_{b1} \cdot \omega_1} \int_{\xi A}^{\xi_E} Q_{f,th1}(\xi) \ \mathrm{d}\xi \tag{14a}$$

$$\hat{Q}_{f,1} = \frac{z_1}{t_1} \cdot E_{f,th1} \tag{14b}$$

Equations (14a) and (14b) can be easily adapted to determine the frictional heat and the average frictional thermal power entering the wheel.

Calculation of the heat partition factor can be tackled down in different ways, and Gurskii [42] provides a good review of them. Among these methods, it can be said that the most relevant is the one proposed by Blok [3], which consists on the application of the following equation:

$$\varphi(\xi) = \frac{e_1 \cdot \sqrt{v_{r1}(\xi)}}{e_1 \cdot \sqrt{v_{r1}(\xi)} + e_2 \cdot \sqrt{v_{r2}(\xi)}} \tag{15}$$

where $v_{r1}(\xi)$ is the rolling speed of the pinion, $v_{r2}(\xi)$ is the rolling speed of the wheel and e_1 and e_2 are the thermal effusivities of pinion and wheel, respectively.

3.2. Common simplifications and other considerations

One of the main advantages of the analytical methods is that they usually offer an easy solution to a complex problem. Such an easy solution comes from the adoption of some simplifying assumptions, which in some cases reduce the accuracy of the method. In the case of the analytical methods for the calculation of the bulk temperature of polymer gears, these simplifications mostly affect the prediction of the coefficient of friction and the load sharing function.

The prediction of coefficient of friction and its variation along the line of action is well established for gears operating under elastohydrodynamic lubrication [43–48], but only a small number of works can be found related to the prediction of the coefficient of friction for polymer gear pairs [49–52]. Nevertheless, a common assumption in the models that constitute the scope of this work [5, 30, 36] is to consider that the coefficient of friction has a constant magnitude along the line of action, in such a way that $\mu(\xi) = \mu$. This assumption allow us to rewrite Eq. (11) as:

$$\hat{Q}_f = \mu \cdot P_{in} \cdot H_V \tag{16}$$

where H_V is defined as the degree of tooth loss [53]:

$$H_V = \frac{1}{p_b} \cdot \int_{\xi_A}^{\xi_E} \frac{\beta(\xi) \cdot v_s(\xi)}{v_n} \, \mathrm{d}\xi \tag{17}$$

The previous equation includes the load sharing function $\beta(\xi)$, which in the case of polymer gear transmissions takes complex shapes [54, 55]. To provide an example, Fig. 2a shows the load sharing function for a polymer gear pair, calculated using the finite element model described in Ref. [14]. To avoid this complexity and assuming a perfect load sharing between teeth, in the great majority of the cases the load sharing function is approached to a stepped function, as the one shown in Fig. 2b.

Figure 2 also allows us to observe another important phenomena that affects the heat generation by sliding friction in polymer gear transmissions: the contact out of the line of action. As it has already been reported by several authors [56–58], polymer gears are

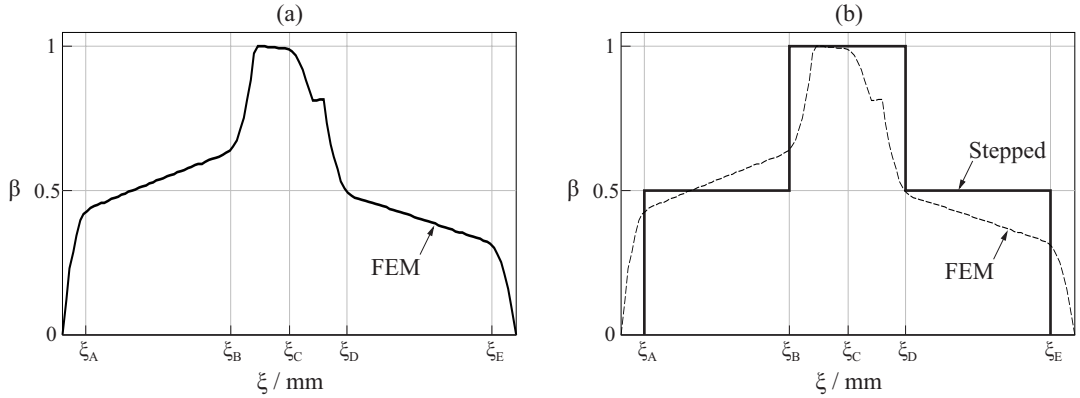

Figure 2: Load sharing functions: (a) FEM model according to [14] and (b) rigid model vs. FEM.

subjected to large deflections that can cause a premature contact occurring before the theoretical initial point of contact (denoted by ξ_A in Fig. 2) and an extended contact after the theoretical end of the contact (denoted by ξ_E in Fig. 2). Out of the line of action, contact typically occurs at the tip of the pinion and wheel teeth, where maximum rates of heat generation are produced [14]. For this reason, this phenomenon can have an important repercussion over the operating temperature of the gears. Although some efforts have been made to consider the side-effects of the contact out of the line of action [38], they are neglected in the analytical methods that constitute the scope of this work.

Following the previous assumptions (a constant coefficient of friction and a stepped load sharing between teeth), several formulas to perform an approximated evaluation of Eq. (17) can be found on the literature [43, 59, 60], which are analyzed and compared in Ref. [61].

Finally, another common assumption in some of the reviewed methods [5, 22] is the use of an average heat partition factor $\hat{\varphi}$. This averaged heat partition factor can be calculated as the ratio between the average frictional thermal power entering the pinion and the total thermal power generated by friction. Considering Eq. (16), the following relation holds:

$$\hat{\varphi} = \frac{\hat{Q}_{f,1}}{\hat{Q}_f} \rightarrow \hat{Q}_{f,1} = \mu \cdot P_{in} \cdot H_V \cdot \hat{\varphi} \tag{18}$$

4. Heat generated by hysteresis losses

Figure 3 summarizes the application of the Kelvin-Voigt rheological model for the determination of the response of a gear tooth made of viscoelastic material [30]. The gear tooth is referred to an inertial coordinate frame that is rigidly connected to the gear, in such a way that its rigid body motions are neglected. The behavior of the tooth under load is represented by a viscous damper (with damping coefficient c) and an elastic spring (with elastic coefficient k), which are connected in parallel and aligned in the direction of the line of action. A force F_n is applied at point Y in the direction of the line of action and the response of the system, in terms of displacement u and velocity $\dot{u}$ of the point Y, is given by the following differential equation:

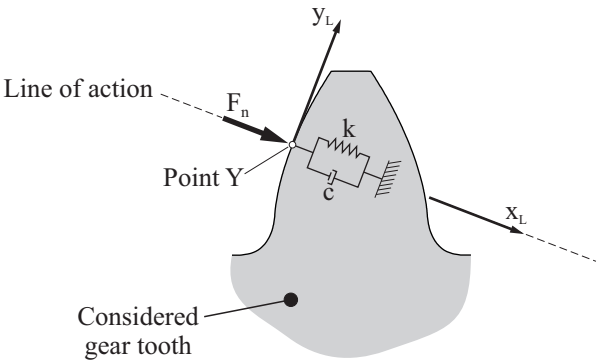

Figure 3: Kelvin-Voigt rheological model

$$k \cdot u + c \cdot \dot{u} = F_n \tag{19}$$

This differential equation does not have a general closed-form solution, but it can be solved using numerical methods such as the Runge-Kutta [62]. However, closed-form solutions are preferred to be used in analytical methods to calculate the bulk temperature of polymer gears, because they are faster and easier to implement. For these reasons, it is common to make some simplificative assumptions under which it is possible to obtain a closed-form solution for Eq. 19. In this line, considering k, c and F_n constant along the line of action, and assuming $u(0) = 0$, a closed-form solution for Eq. 19 can be obtained as:

$$\dot{u}(t) = \frac{F_n}{c} \cdot e^{-k \cdot t/c} \tag{20}$$

Considering this closed-form solution, the instantaneous power dissipated by the viscous damper can be calculated as:

$$Q_h(t) = c \cdot \dot{u}(t) \cdot \dot{u}(t) = \frac{F_n^2}{c} \cdot e^{-2 \cdot k \cdot t/c} \tag{21}$$

Finally, and assuming that all the hysteresis power losses are dissipated as heat, the hysteretic heat generated over a period of time of duration Δt is calculated as:

$$E_h = \int_0^{\Delta t} Q_h(t)\ \mathrm{d}t = \frac{F_n^2}{2 \cdot k} \cdot \left(1 - e^{-2 \cdot k \cdot \Delta t/c}\right) \tag{22}$$

Stiffness coefficient k represents the single tooth stiffness and accounts for the deformations produced by the contact and the bending of the tooth. Several authors [20, 38] have reported that hysteresis produced by bending is small compared to the one produced by contact deformation. Based on this hypothesis, other methods [32, 38] have been derived for the determination of the hysteresis heat, considering only the contact deformation and neglecting the bending of the tooth.

5. Heat dissipated by convection: Newton's law of cooling

Despite the complexity of this phenomenon, the heat dissipated by convection is observed to be proportional to the difference between the temperature of the surface T and the temperature of the surrounding air sufficiently far from the surface T_∞. This behaviour is conveniently expressed by Newton's law of cooling as:

$$\hat{Q}_c = h_c \cdot A_c \cdot (T - T_\infty) \tag{23}$$

where h_c is the convective heat transfer coefficient and A_c is the area of the surface through which convection heat transfer takes place.

The convective heat transfer coefficient is not a material property and needs to be determined from experimental analyses. It depends on the geometry of the body, the thermal properties of the fluid and the relative motion between the fluid and the studied body. The heat transfer coefficient is often calculated as:

$$h_c = Nu \cdot \frac{\lambda_{air}}{L_c} \tag{24}$$

where λ_{air} is the thermal conductivity of the surrounding air, L_c represents the characteristic length of the observed surface and Nu is the Nusselt number. For forced convection, the Nusselt number is generally a function of the Reynolds number Re and the Prandtl number Pr, which can be expressed as:

$$Nu = C_1 \cdot Re^{C_2} \cdot Pr^{C_3} \tag{25}$$

where C_1, C_2 and C_3 are constants to be determined experimentally for each particular geometry and boundary conditions [40]. Substituting Eq. (25) into Eq. (24) and considering the definitions for the Reynolds and the Prandtl numbers, the following equation is obtained for the heat transfer coefficient:

$$h_c = C_1 \cdot \frac{\lambda_{air}}{L_c} \cdot \left(\frac{v_{air} \cdot L_c}{\nu_{air}} \right)^{C_2} \cdot \left(\frac{\nu_{air}}{\alpha_{air}} \right)^{C_3} \tag{26}$$

where v_{air} is the relative speed of the air with respect to the observed surface, and ν_{air} and α_{air} are the kinematic viscosity and the thermal diffusivity of the surrounding air, respectively.

6. Hachmann and Strickle method and its application in VDI 2376 Standard

Figure 4 shows the thermal model proposed by Hachmann and Strickle [22], which consists of a gear case and the considered polymer gear (either the pinion or the wheel). In this model, the corresponding part of the heat generated by friction ($\hat{Q}_{f,1}$) is released over the polymer gear, which remains at a temperature T. Since thermal equilibrium must be fulfilled, the frictional heat released over the selected gear must be dissipated by convection to the air within the gear case ($\hat{Q}_{f,1} = \hat{Q}_{c,V}$), which remains at a temperature T_i. Finally,

this heat is dissipated by convection to the ambient air ($\hat{Q}_{c,V} = \hat{Q}_{c,Vg}$), which remains at a temperature T_∞. The following equation holds:

$$\hat{Q}_{f,1} = \hat{Q}_{c,V} = \hat{Q}_{c,Vg} \tag{27}$$

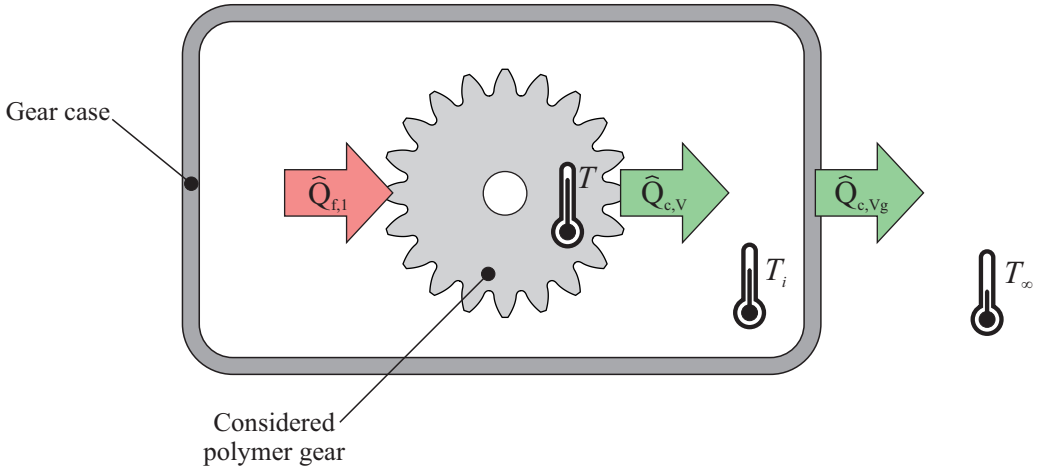

Figure 4: Thermal model considered by Hachmann and Strickle

6.1. Heat generation model

Hachmann used Eq. (18) to calculate the average frictional thermal power entering the pinion. In this case, the degree of tooth loss (given by Eq. (17)) was approximated as [63]:

$$H_V = 2.6 \cdot \frac{z_1 + z_2}{z_1 \cdot (z_2 + 5)} \tag{28}$$

The previous equation was derived for a standard spur gear pair, with a pressure angle of 20° and no profile shift coefficients. In order to enable the application of this temperature calculation method to other gear geometries, the VDI 2736 standard approximates the degree of tooth loss using the following equation [59]:

$$H_V = \frac{\pi \cdot (z_1 + z_2)}{z_1 \cdot z_2 \cdot \cos \beta_b} \cdot \left(1 - \varepsilon_1 - \varepsilon_2 + \varepsilon_1^2 + \varepsilon_2^2\right) \tag{29}$$

where ε_1 and ε_2 are the partial contact ratios and β_b is the base helix angle (for helical gears). By replacing Eq. (28) with Eq. (29) in the calculation of the average frictional thermal power entering the pinion, it is possible to consider gear modifications, different axis distances, and to calculate the degree of tooth loss for helical gears.

Replacing Eq. (29) into Eq. (18), the following equation is obtained for the calculation of the average frictional thermal power entering the pinion:

$$\hat{Q}_{f,1} = \mu \cdot P_{in} \cdot \frac{\pi \cdot (z_1 + z_2)}{z_1 \cdot z_2 \cdot \cos \beta_b} \cdot \left(1 - \varepsilon_1 - \varepsilon_2 + \varepsilon_1^2 + \varepsilon_2^2\right) \cdot \hat{\varphi} \tag{30}$$

6.2. Heat dissipation model

As it is reflected in Fig. 4, Hachmann's heat dissipation model takes into account the heat dissipated from the polymer gear to the air within the gear case, and the dissipation of this heat to the ambient air. Both convection phenomena are modeled using Newton's law of cooling (see section 5), in such a way that setting $\hat{Q}_{c,V} = \hat{Q}_{c,Vg}$ and solving for $\hat{Q}_{c,V}$ the following equation is obtained:

$$\hat{Q}_{c,V} = (T - T_\infty) \cdot \left(\frac{1}{h_{c,V} \cdot A_{c,V}} + \frac{1}{h_{c,Vg} \cdot A_{c,Vg}} \right)^{-1} \tag{31}$$

Here, $A_{c,V}$ is the convective area and $h_{c,V}$ is the convective heat transfer coefficient for the polymer gear, and they constitute the heat dissipation model of the gear. On the other hand, $A_{c,Vg}$ is the convective area and $h_{c,Vg}$ is the convective heat transfer coefficient for the gear case.

To develop the heat dissipation model of the polymer gear, each tooth of the gear is approached to a plate of width b and height $k_1 \cdot m$, and the gear is substituted by a set of z rotating plates. By doing so, the convective area of the gear is:

$$A_{c,V} = z \cdot k_1 \cdot m \cdot b \tag{32}$$

where k_1 is an empirical coefficient to adjust the size of the convective area. On the other hand, the convective heat transfer is calculated using Eq. (26), assuming that the characteristic length of the plates is $L_c = \pi \cdot m$ and setting $C_2 = C_3 = 3/4$:

$$h_{c,V} = C_1 \cdot \frac{\lambda_{air}}{\pi \cdot m} \cdot \left(\frac{v_{air} \cdot \pi \cdot m}{\nu_{air}} \right)^{3/4} \cdot \left(\frac{\nu_{air}}{\alpha_{air}} \right)^{3/4} \tag{33a}$$

$$h_{c,V} = \frac{C_1 \cdot \pi^{3/4}}{\pi} \cdot \frac{\lambda_{air}}{m} \cdot \left(\frac{v_{air} \cdot m}{\alpha_{air}} \right)^{3/4} \simeq \frac{1}{20} \cdot \frac{\lambda_{air}}{m} \cdot \left(\frac{v_{air} \cdot m}{\alpha_{air}} \right)^{3/4} \tag{33b}$$

Substituting Eq. (33b) and Eq. (32) into Eq. (31), the following equation is obtained for the convective heat dissipation of the polymer gear:

$$\hat{Q}_{c,V} = (T - T_\infty) \cdot \left(\frac{20 \cdot \alpha_{air}^{3/4}}{k_1 \cdot b \cdot z \cdot \lambda_{air} \cdot (v_{air} \cdot m)^{3/4}} + \frac{1}{h_{c,Vg} \cdot A_{c,Vg}} \right)^{-1} \tag{34}$$

For comparison purposes, an additional magnitude $\hat{q}_{c,V}$ is derived from Eq. (31), which represents the heat convection per temperature change for the observed polymer gear and it is calculated as follows:

$$\hat{q}_{c,V} = \frac{\hat{Q}_{c,V}}{T - T_\infty} = \left(\frac{20 \cdot \alpha_{air}^{3/4}}{k_1 \cdot b \cdot z \cdot \lambda_{air} \cdot (v_{air} \cdot m)^{3/4}} + \frac{1}{h_{c,Vg} \cdot A_{c,Vg}} \right)^{-1} \tag{35}$$

6.3. Temperature calculation model

By replacing Eq. (30) and Eq. (34) into Eq. (27) the following equation is obtained for the calculation of the temperature of a polymer gear:

$$T = T_\infty + \mu \cdot P_{in} \cdot H_V \cdot \left(\frac{k_\vartheta}{b \cdot z \cdot (v_{air} \cdot m)^{3/4}} + \frac{R_{\lambda,G}}{A_{c,Vg}} \right) \cdot ED^{0.64} \tag{36}$$

where $R_{\lambda,G} = \frac{\hat{\varphi}}{h_{c,Vg}}$ and k_ϑ is defined as:

$$k_\vartheta = \frac{20 \cdot \hat{\varphi} \cdot \alpha_{air}^{3/4}}{k_1 \cdot \lambda_{air}} \tag{37}$$

The previous equation also includes the term $ED^{0.64}$, which is aimed to consider the transient thermal behavior of the polymer gear pair. Here, ED is the relative tooth-engagement time, as defined in Ref. [64], which varies between 0 and 1.

Using Eq. (36), the temperature T can be determined both for the flank or root position by choosing the adequate k_ϑ and $R_{\lambda,G}$ factors as presented in Ref. [5]. Here it is important to mention that, as explained by Houz [7], the flank temperature estimated using this method represents the mean temperature integrated along the length of the flank, and it should not be confused with the maximum instantaneous flash temperature. In this work, which is focused on the calculation of the bulk temperature, heat transfer coefficients k_ϑ for root position will be used.

6.4. Remark on the average heat partition factor in VDI 2736 standard

Table 1 shows the values proposed by VDI 2736 standard [5] for heat transfer coefficient k_ϑ at the root of the tooth. As reflected in Eq. (37), this coefficient is dependent on the average heat partition factor $\hat{\varphi}$ and on the empirical coefficient k_1, whose values are not given explicitly in VDI 2736 standard. In this section, some inferences are made to obtain reference values for these coefficients, in order to provide a better understanding of the performance of the method.

Table 1: Guide values for dry-running gears according to VDI 2736 [5].

Pairing	k_ϑ root	k_1	$\hat{\varphi}$
Polymer/polymer	$2148\,\mathrm{K(m/s)^{0.75}mm^{1.75}/W}$	10.16	0.50
Polymer/steel	$895\,\mathrm{K(m/s)^{0.75}mm^{1.75}/W}$	10.16	0.21

Let us first consider a polymer gear transmission in which the pinion and the wheel are made of the same material. Assuming that the pinion and the wheel have the same geometry, then the average heat partition factor is $\hat{\varphi} = 0.5$. In this case, solving Eq. 37 for k_1, and considering the magnitude for k_ϑ shown in Tab. 1, together with the typical magnitudes for λ_{air} and α_{air}, it is obtained that $k_1 \simeq 10.16$.

Now, let us consider a gear transmission in which the pinion and the wheel are made from different materials. Note that the calculated coefficient k_1 should not vary with the material combination of the gear pair. Solving Eq. 37 for $\hat{\varphi}$, and considering the magnitude for k_ϑ shown in Tab. 1, the average heat partition factor for polymer/steel gear pairs is $\hat{\varphi} \simeq 0.21$.

Finally, it is important to remark that the estimated values for k_1 and $\hat{\varphi}$ does not affect the accuracy of the method, as they are already implicit in the provided values of k_ϑ.

7. Takanashi and Shoji method

Figure 5 shows the thermal model proposed by Takanashi [29, 30]. In this model, the thermal system is composed by a gear tooth. The corresponding part of the heat generated by friction ($E_{f,th1}$) and the heat generated by hysteresis ($E_{h,th1}$) are released over the gear tooth, which remains at a temperature T. Since thermal equilibrium must be guaranteed, this heat is entirely dissipated by convection to the surrounding air, which remains at a temperature T_∞. The following equation holds:

$$E_{f,th1} + E_{h,th1} = E_{c,T} \tag{38}$$

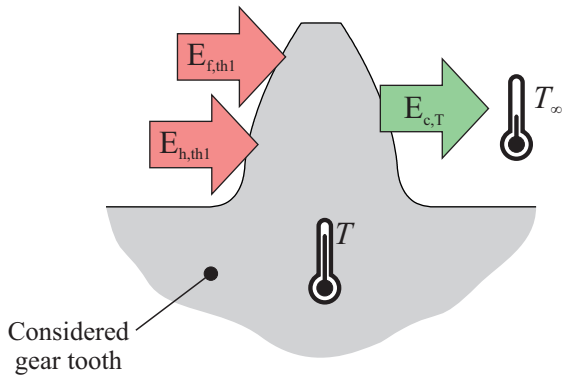

Figure 5: Thermal model considered by Takanashi

7.1. Heat generation model

For the calculation of the frictional heat entering the pinion tooth, Takanashi relies on the application of Eq. (14a) in combination with Blok's definition for the heat partition factor (given by Eq. (15)). The integral present in Eq. (14a) is evaluated dividing the domain (segment AE over the line of action) into four intervals $i = [AB, BC, CD, DE]$ (Figs. 1 and 2). Then, considering a constant coefficient of friction throughout the line of action and using the midpoint integration rule, the following equation is obtained:

$$E_{f,th1} = \mu \cdot F_{bn} \cdot \sum_i \beta_i \cdot v_{s,i} \cdot \varphi_i \cdot \Delta t_i \tag{39}$$

where β_i, $v_{s,i}$ and φ_i are the load sharing factor, the sliding speed and the heat partition coefficient at the middle of the considered segment i, respectively. On the other hand, Δt_i is the duration of the contact in such a segment.

To enable the comparison between models, the average frictional thermal power entering the pinion is calculated from $E_{f,th1}$ as described by Eq.(14b):

$$\hat{Q}_{f,1} = \frac{z_1}{t_1} \cdot E_{f,th1} = \frac{z_1}{t_1} \cdot \left[\mu \cdot F_{bn} \cdot \sum_i \beta_i \cdot v_{s,i} \cdot \varphi_i \cdot \Delta t_i \right] \tag{40}$$

For the calculation of the heat generated by hysteresis, Takanashi also divides the line of action into four intervals $i = [AB, BC, CD, DE]$. For each one of these intervals, Eq. (22) is applied considering that the stiffness, the damping coefficient and the applied force remain constant during all the interval. It must be emphasized that this assumption is important in order to obtain a closed form solution for Eq. (19). By doing so, the following equation is obtained:

$$E_{h,th1} = \frac{F_{bn}^2}{2} \cdot \sum_i \frac{\beta_i^2}{k_i} \cdot \left(1 - e^{-2 \cdot k_i \cdot \Delta t_i / c_i}\right) \tag{41}$$

where k_i and c_i are the single tooth stiffness and the average damping coefficient at interval i, respectively. Takanashi provides a simple method for the calculation of the single tooth stiffness, which is based on the works of Timoshenko [65] and Caldwell [66]. Other enhanced methods can be found in the literature for the calculation of the single tooth stiffness [67, 68], and a good review of them is provided in Ref. [69]. However, it is important to mention that the great majority of these methods are based on the small strain elasticity theory, and their validity for polymer gears (which usually undergo large deformations) has not been tested. Finally, Tab. 2 provides some reference values for the damping coefficient c, extracted from Ref. [49].

Table 2: Guide values for damping coefficient per unit face width c_i/b / N s/mm^2 [49].

Temperature	PA6	POM
15 °C	0.796	0.396
30 °C	1.245	0.482
45 °C	1.874	0.525

7.2. Heat dissipation model

In Takanashi's model, the heat dissipated by convection from the considered gear tooth, during a revolution of the pinion whose duration is given by t_1, can be calculated considering Eq. (23) as:

$$E_{c,T} = \hat{Q}_{c,T} \cdot t_1 = h_{c,T} \cdot A_{c,T} \cdot (T - T_\infty) \cdot t_1 \tag{42}$$

where $A_{c,T}$ and $h_{c,T}$ are the convective area and heat transfer coefficient of the gear tooth, respectively. In Takanashi's original model [30], the convective heat transfer coefficient is calculated using Eq. (26), assuming that the characteristic length of the plate is $L_c = m$, $C_1 = 1.75 \cdot \left(\frac{m}{b}\right)^{1.5}$, $C_2 = 0.45$ and $C_3 = 0.4$:

$$h_{c,T} = \left[1.75 \cdot \left(\frac{m}{b}\right)^{1.5}\right] \cdot \frac{\lambda_{air}}{m} \cdot \left(\frac{m \cdot v_{air}}{\nu_{air}}\right)^{0.45} \cdot \left(\frac{\nu_{air}}{\alpha_{air}}\right)^{0.4} \tag{43}$$

More recently, Takanashi has provided different definitions for the convective heat transfer coefficient [31, 32], with different magnitudes for constants C1, C2 and C3. In a recent book, Erhard [33] provided the following equation for the heat transfer coefficient in Takanashi's model, which is the one considered in this work:

$$h_{c,T} = \frac{\lambda_{air}}{m} \cdot \left(\frac{m}{b}\right)^{0.05} \cdot \left(\frac{m \cdot v_{air}}{\nu_{air}}\right)^{0.4} \tag{44}$$

Neither Takanashi [30–32] nor Erhard [33] provide further details on how to calculate the convective area of the gear tooth $A_{c,T}$. However, making an analogy to the convection of plates theory the area for a gear tooth would be:

$$A_{c,T} = b \cdot (r_a - r_f) \tag{45}$$

where r_a and r_f are the tip and the root radius of the gear, respectively.

For comparison purposes, an additional magnitude $\hat{q}_{c,T}$ is derived from Eq. (42), which represents the heat convection per temperature change for the observed polymer gear, and it is calculated as:

$$\hat{q}_{c,T} = z_1 \cdot \frac{\hat{Q}_{c,T}}{T - T_\infty} = z_1 \cdot \left[b \cdot (r_a - r_f) \cdot \frac{\lambda_{air}}{m} \cdot \left(\frac{m}{b}\right)^{0.05} \cdot \left(\frac{m \cdot v_{air}}{\nu_{air}}\right)^{0.4}\right] \tag{46}$$

Since Takanashi's model was derived to calculate the heat dissipated by convection from a single gear tooth, the factor z_1 is introduced in the previous equation to calculate the heat dissipated by convection by the whole pinion.

7.3. Temperature calculation model

By replacing Eq. (42) into Eq. (38) the following equation is obtained for the calculation of the temperature of a polymer pinion:

$$T = T_\infty + \frac{E_{f,th1} + E_{h,th1}}{h_{c,T} \cdot A_{c,T} \cdot t_1} \tag{47}$$

where $E_{f,th1}$ and $E_{h,th1}$ are calculated according to Eq. (39) and Eq. (41), respectively.

8. Mao and Hooke method

Figure 6 shows the thermal model proposed by Mao and Hooke [36]. In this model the thermal behaviour of the polymer gear pair is approximated to that of a gear pump. During the operation of this gear pump, pockets of air are trapped between the gear teeth, which are carried around and heated as the gears rotate. This warm air is expelled as the gears mesh and it is replaced by cold air as the teeth pull apart.

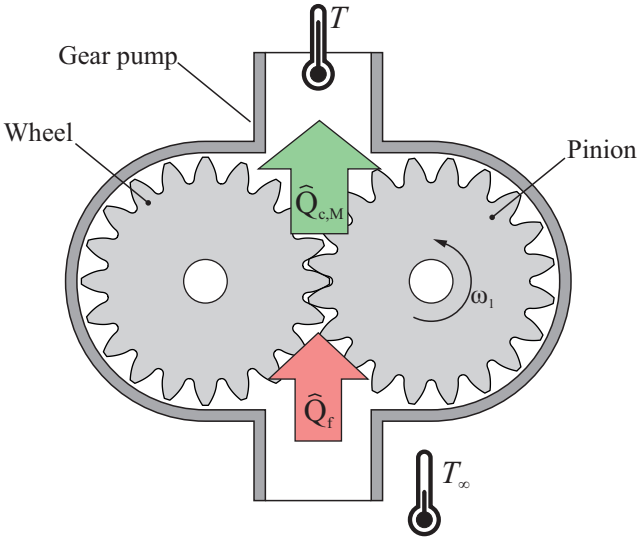

Figure 6: Thermal model considered by Mao

Mao model was developed under the assumption that the pinion and the wheel are identical (same geometry and same material). Besides that, Mao assumed that the air that is trapped within each tooth pocket reaches a temperature close to that of the gear surfaces, and that no heat is lost by convection from the open ends. Turbulence within each pocket will ensure that the non-contacting gear surface is heated to a temperature close to that of the contacting surfaces.

Thus, the average frictional thermal power ($\hat{Q}_f$) is released over the polymer gears, increasing their temperature. To satisfy the thermal equilibrium, this heat is transferred from the gears to the air that is trapped in the pockets between their teeth. When this air is expelled from the gear pump, heat ($\hat{Q}_{c,M}$) is removed, so the following equation holds:

$$\hat{Q}_f = \hat{Q}_{c,M} \tag{48}$$

8.1. Heat generation model

The average frictional thermal power $\hat{Q}_f$ is calculated following the definition provided by Eq. (16). Performing a similar approach to that taken by Ohlendorf [59], but specified for a spur gear transmission in which the pinion and the wheel have the same number of teeth ($z_1 = z_2 = z$), the degree of tooth loss is given by:

$$H_V = \frac{\pi}{z} \cdot \left(\varepsilon_\alpha^2 - 2 \cdot \varepsilon_\alpha + 2\right) \tag{49}$$

By doing an additional assumption in which $\varepsilon_\alpha = 1.5$, Mao was able to simplify the previous equation to:

$$H_V = \frac{1.25 \cdot \pi}{z} \tag{50}$$

Replacing Eq. (50) into Eq. (16), the following equation is obtained for the calculation of the average frictional thermal power:

$$\hat{Q}_f = \mu \cdot P_{in} \cdot \frac{1.25 \cdot \pi}{z} \tag{51}$$

To enable the comparison between models, the average frictional thermal power entering the pinion is calculated as described by Eq.(18):

$$\hat{Q}_{f,1} = \mu \cdot P_{in} \cdot H_V \cdot \hat{\varphi} = \mu \cdot P_{in} \cdot \left[\frac{1.25 \cdot \pi}{z}\right] \cdot \frac{1}{2} \tag{52}$$

Here, it is worth emphasizing that Mao's model considers that both pinion and wheel are identical (same geometry and same material). For this reason, it is fair to assume that frictional heat is evenly distributed between both gears, thus imposing an average heat partition factor $\hat{\varphi} = 1/2$ in Eq. (52).

8.2. Heat dissipation model

The amount of heat dissipated by convection can be determined by considering the heat capacity of the displaced air:

$$\hat{Q}_{c,M} = \frac{\mathrm{d}m_{air}}{\mathrm{d}t} \cdot cp_{air} \cdot (T - T_\infty) \tag{53}$$

where $\frac{\mathrm{d}m_{air}}{\mathrm{d}t}$ is the mass rate of displaced air, cp_{air} is the specific heat of the air, T is the temperature of the air, and T_∞ is the temperature of the fluid sufficiently far from the gear surface. The mass rate of displaced air can be expressed as:

$$\frac{\mathrm{d}m_{air}}{\mathrm{d}t} = \omega \cdot V_{air} \cdot \rho_{air} \tag{54}$$

where ω is the rotating speed of the gears, ρ_{air} is the density of the air and V_{air} is the volume of air expelled in each revolution:

$$V_{air} = 2 \cdot b \cdot \pi \cdot \left(r_a^2 - r^2\right) \tag{55}$$

where b is the face width of the gears, r_a is the tip radius and r is the reference radius of the gear. Considering the previous equations, the amount of heat dissipated by convection can be calculated as:

$$\hat{Q}_{c,M} = \omega \cdot 2 \cdot b \cdot \pi \cdot \left(r_a^2 - r^2\right) \cdot \rho_{air} \cdot cp_{air} \cdot (T - T_\infty) \tag{56}$$

For comparison purposes, the heat convection per temperature change for the observed polymer gear ($\hat{q}_{c,M}$) is derived from Eq. (53), and it is calculated as:

$$\hat{q}_{c,M} = \frac{1}{2} \cdot \frac{\hat{Q}_{c,M}}{T - T_\infty} = \frac{1}{2} \cdot \left[\omega \cdot 2 \cdot b \cdot \pi \cdot \left(r_a^2 - r^2\right) \cdot \rho_{air} \cdot cp_{air}\right] \tag{57}$$

Here, a factor of 1/2 is introduced because in Mao's model the magnitude $\hat{Q}_{c,M}$ corresponds to the heat dissipated from the gear pair. Since in this model it is assumed that both gears are identical, it is reasonable to assume that the heat dissipated from one gear is half the heat dissipated from the gear pair.

8.3. Temperature calculation model

By replacing Eq. (51) and Eq. (56) into Eq. (48), the following equation is obtained for the calculation of the temperature of a polymer gear pair:

$$T = T_\infty + \frac{0.625 \cdot \mu \cdot M_1}{cp_{air} \cdot \rho_{air} \cdot z \cdot b \cdot (r_a^2 - r^2)} \tag{58}$$

Note that the previous equations implies that the temperature of the gears is not dependent on the rotating speed of the gears. Compared to Takanashi and Mao methods, the main advantage of this method is that it does not require the calculation of a heat transfer coefficient, as Mao's heat dissipation model is not based on Newton's law of cooling. The main drawback is that it can only be successfully applied to polymer gear transmissions in which both gears are identical. Moreover, the simplifications made to calculate the degree of tooth loss (Eq. (50)) can introduce errors when $\varepsilon_\alpha \neq 1.5$. Finally, it is important to mention that Mao uses a different version of the previous equation in some works [19, 70, 71], where the coefficient 0.625 is replaced by 3.927, although no further explanations are given for this change.

9. Numerical examples and discussion

A set of case studies were selected from the literature in order to test the presented methods and compare them with available experimental results [27, 37, 72]. The gear geometries, materials and operating conditions that define the case studies are listed on Tab. 3. The case studies are identified according to the original source: case study GP (Gear Pogačnik, extracted from [27]), case study GS (Gear Singh, extracted from [37]) and case study GL (Gear Letzelter, extracted from [72]).

The case studies were selected to cover a wide range of polymer gear applications, ensuring a variety of geometrical parameters (module, teeth number and face width) and operating conditions (input speeds, input torques, ambient temperatures and coefficients of friction). The selected case studies also cover typical material pairing combinations like polymer/steel and polymer/polymer. In this line, three typical thermoplastics used for gear applications

Table 3: Definition of case studies: gear geometries, materials and operating conditions

Parameter	GP [27]	GS [37]	GL [72]
Normal module, m_n/mm	1	2	3
Normal pressure angle, α_n/°	20	20	20
Face width, b/mm	6	8	20
Pinion tooth number, z_1	20	20	32
Wheel tooth number, z_2	20	20	41
Pinion material	POM	POM	PA66
Wheel material	PA6	Steel	PA66
Working axis distance, a_w/mm	20.05	40.00	78.00
Nominal input speed, ω_1/rpm	1646	1200	600
Nominal input torque, M_1/N m	0.59	2.0	10.0
Ambient temperature, T_∞/°C	23	29	21
Coefficient of friction, μ	0.18 [5]	0.20 [5]	0.40 [5]

*All open gear transmissions

are studied: polyoxymethylene (POM), polyamide-6 (PA6) and polyamide-66 (PA66). The material thermal properties are summarized in Tab. 4. The air properties considered for the calculations are given in Tab. 5.

Table 4: Thermal properties of the gear materials [5]

Property	Steel	POM	PA66	PA6
Density, ρ/kg/m^3	7850	1410	1145	1135
Thermal conductivity, λ/W/(m K)	52	0.28	0.23	0.29
Specific heat, cp/J/(kg K)	470	1470	1670	1500

In the following subsections the frictional heat generation, the hysteretic heat generation and the convective heat dissipation models of the selected methods are studied. Finally, the temperature prediction models of these methods are assessed.

9.1. Heat generated by sliding friction

In this subsection the frictional heat generation models of the selected methods (VDI 2736, Mao and Takanashi) are compared between them in terms of the average frictional thermal power entering the pinion ($\hat{Q}_{f,1}$) predicted for each case study of Tab. 3. Additionally, and with the aim of being used as a reference values, theoretical results are also included in this comparison.

To obtain these theoretical results, the instantaneous frictional power loss ($Q_{f,th}$) is calculated for each case study using Eq. (9). Then, taking into consideration the instantaneous

Table 5: Thermal properties of the surrounding air at different temperatures

Property	21 °C	23 °C	29 °C
Thermal conductivity, λ_{air}/W/(m K)	25.76×10^{-3}	25.91×10^{-3}	26.35×10^{-3}
Kinematic viscosity, ν_{air}/m^2/s	15.43×10^{-6}	15.62×10^{-6}	16.18×10^{-6}
Specific heat, cp_{air}/J/(kg K)	1006.84	1006.92	1007.16
Density, ρ_{air}/kg/m^3	1.185	1.177	1.154

heat partition factor, the thermal power entering the pinion tooth ($Q_{f,th1}$) is calculated according to Eq. (13). Both magnitudes are shown in Fig. 7 for each case study, illustrating the effect of the heat partition factor. From these results, the theoretical values for $\hat{Q}_{f,1}$ are obtained using Eq. (14b), where $E_{f,th1}$ is calculated by numerical integration of Eq. (14a). Finally, the theoretical average heat partition factor ($\hat{\varphi}$) is calculated according to the definition provided by Eq. (18). The resulting values for $\hat{Q}_{f,1}$ and $\hat{\varphi}$ are reflected in Tab. 6.

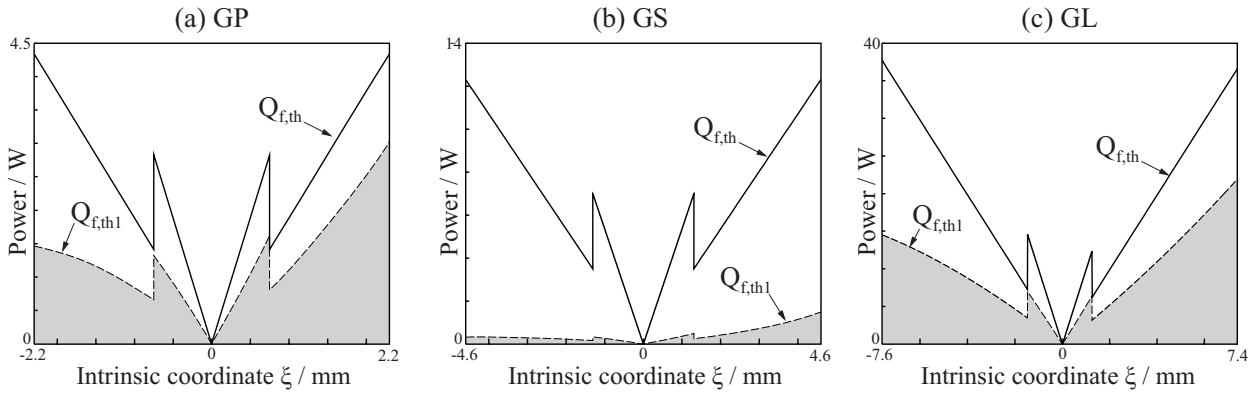

Figure 7: Theoretical instantaneous frictional power loss for case studies GP, GS and GL

Table 6 also includes the resulting values for $\hat{Q}_{f,1}$ and $\hat{\varphi}$ as calculated by VDI 2736, Mao and Takanashi methods. In VDI 2736 standard, the average frictional thermal power entering the pinion is calculated using Eq. (30). This equation contains an average heat partition factor that is implicitly included in VDI 2736 formulation (see section 6.4), which is insensitive to the transmission ratio and only implicitly provides values that take into account the material pair. This affects the accuracy in which $\hat{Q}_{f,1}$ is calculated, and explains the differences with respect to the theoretical values observed in Tab. 6. These differences are higher for the case study GS than for the case study GL, showing that in VDI 2736 calculations the deviations from the theoretical results are due to the material pairing other than the transmission ratio.

According to Mao's frictional heat generation model, the average frictional thermal power entering the pinion is calculated using Eq. (52). In this model, the frictional heat is implicitly

Table 6: Frictional heat generation results for case studies GP, GS and GL

Quantity	Theoretical Eq. (14b)	VDI 2736 Eq. (30)	Takanashi Eq. (40)	Mao Eq. (52)	Case study
$\hat{Q}_{f,1}$ / W	1.87	1.81	1.88	1.80	GP
	0.60	2.15	0.58	4.93	GS
	16.07	16.26	16.11	15.42	GL
$\hat{\varphi}$	0.519	0.500*	0.519	0.500*	GP
	0.058	0.208*	0.056	0.500*	GS
	0.494	0.500*	0.495	0.500*	GL

*Implicitly included in the derivation of the method

divided into two equal parts both for pinion and wheel, imposing an average heat partition factor $\hat{\varphi} = 0.5$. As it has already been discussed, this method can only be accurate if the gears have the same geometry and are made from the same material. This is observed in Tab. 6, as Mao's results diverge from the theoretical ones when the previous requirements are not fulfilled.

Finally, Takanashi method is based on the frictional heat entering the pinion tooth, which can be expressed in terms of $\hat{Q}_{f,1}$ using Eq. (40). This method predicts almost the same average heat partition factor as the exact theory integration. The small differences (≤ 3 %) were caused by the usage of the midpoint rule for the integration purposes. In terms of frictional heat generation, Takanashi's method is the one that provides closer results to the theoretical solution.

9.2. Heat generated by hysteresis losses

Hysteretic heat is usually neglected in the analytical methods to predict the temperature of polymer gears, under the assumption that its contribution to the temperature rise is small compared to the effect of the frictional heating. In fact, from the considered methods, only Takanashi's is considering hysteresis' effect over the temperature rise. In this subsection this assumption is examined, as well as the accuracy of Takanashi's solution for the hysteretic heat compared to the theoretical one.

Figure 8 shows the hysteretic heat generated during the meshing of a pair of teeth ($E_{h,th1}$) for each case study under four different operating conditions, according to Takanashi and theoretical methods. The theoretical solution for $E_{h,th1}$ is obtained by solving Eq. (19) using the fourth order Runge-Kutta method [62], and then calculating the hysteretic heat by numerical integration of the hysteretic power loss. This figure also shows the frictional heat generated during the meshing of a pair of teeth ($E_{f,th1}$).

In first place, and taking as a reference the results of the theoretical solution, Fig. 8 reveals that in all the cases Takanashi's method tends to overestimate the theoretical values obtained for $E_{h,th1}$. This happens as a consequence of the simplificative assumptions taken

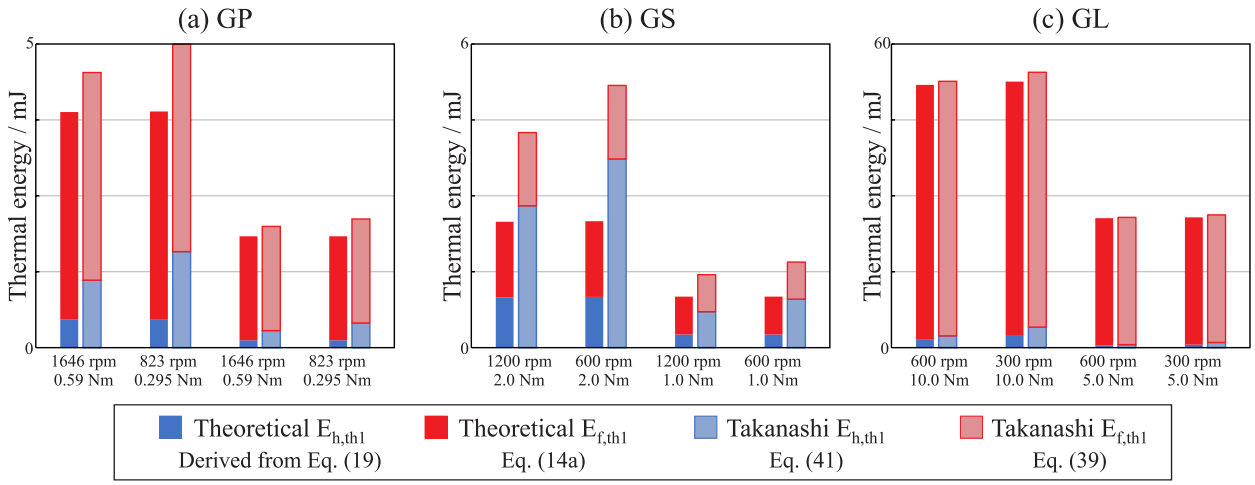

Figure 8: Hysteretic heat generation results for case studies GP, GS and GL

to derive Eq. (41). The minimum relative error between Takanashi and theoretical solutions occurs at case study GL, oscillating between 35% and 75%. The maximum relative error between both methods occurs at case of study GS, oscillating between 173% and 723%.

In second place, the relative contribution of hysteresis to the total heat generated during the meshing of a pair of teeth is examined, taking as a reference the results obtained using Takanashi's method. Here it is important to recall that, as has been shown before, the differences between theoretical and Takanashi frictional heat generation are below 3%. The lowest relative contribution of hysteresis to the total heat is produced for the case study GL (Fig. 8c), where the percentage of heat caused by hysteresis oscillates between 2% and 7%. This is followed by case study GP (Fig. 8a), where hysteretic heat gains relative weight over the frictional heat, but it is still under 32% of the total heat. Finally, for the case study GS (Fig. 8b) the hysteretic heat prevails over frictional heat, reaching 72% of the total heat generated.

The relative weight of hysteresis over the total generated heat is observed to be mostly driven by the coefficient of friction. When the coefficient of friction is large, the relative weight of hysteresis is small because frictional heat has a predominant effect over the generated heat. This is observed in works conducted by Černe [4] and Doll [39], where hysteretic heat oscillates between 0.5% and 5%. On the contrary, when the coefficient of friction is small, hysteretic heat has a larger impact over the total generated heat. This is observed in the work of Takanashi [30], where hysteretic heat reaches rates comprised between 58% and 65% of the total generated heat. These observations indicate that hysteresis could be neglected when the coefficient of friction is large, but it should be taken into account when the coefficient of friction is small.

Figure 8 allows us to draw some other conclusions. Although hysteretic heat increases with the input torque, its relative weight over the total heat decreases as the input torque increases, because frictional heat increases with torque at a higher rate than hysteretic heat. The inverse effect is observed with angular speed: hysteretic heat decreases as the input

speed increases, but its relative weight increases.

Observing Eq. (41), it can also be concluded that hysteretic heat decreases as the damping coefficient and stiffness increase. Moreover, tooth bending stiffness is observed to play a minor role in hysteretic heat generation, compared to contact stiffness. This effect was already reported by Gauvin [20] and Koffi [38].

9.3. Heat dissipated by convection

In this subsection the convective heat dissipation models of the selected methods (VDI 2736, Mao and Takanashi) are compared between them in terms of the heat convection per temperature change ($\hat{q}_c$) predicted for each case study of Tab. 3. For such a purpose, Tab. 7 presents a comparison of the values of $\hat{q}_c$ calculated using the three selected methods, considering the nominal operating conditions. In this case, there is no theoretical solution whose values can serve as reference results.

Table 7: Convective heat dissipation results for case studies GP, GS and GL

Quantity	VDI 2736 Eq. (35)	Takanashi Eq. (46)	Mao Eq. (57)	Case study
$\hat{q}_c$ / W/°C	0.042	0.042	0.081	GP
	0.123	0.088	0.308	GS
	0.776	0.432	1.399	GL

While frictional heat generation is similar among methods, Tab. 7 shows that the heat convection is quite different. Mao's method always presents larger values, which means that using this method, the predicted temperature is typically lower than using the other methods. In the same way, Takanashi's method always has the lowest values, meaning that it typically predicts a larger operating temperature. For the calculation of VDI 2736 convection, it has been considered that $1/h_{c,Vg} = 0$, as the gears are operating under open air conditions.

Figure 9 presents the influence of the angular speed on the convective heat dissipation for each method. The heat convection of the Mao method is linearly dependent on the angular speed. Both Takanashi and VDI 2736 change its heat convection as the Reynolds number changes. Therefore, the heat transfer due to convection is mainly affected by the Reynolds exponents (0.4 vs. 0.75). A smaller exponent on the Reynolds number (Takanashi) implies a larger convection at low speeds but a smaller one at higher speeds.

9.4. Temperature and experimental comparison

In this subsection the temperature calculation models of the selected methods (VDI 2736, Mao and Takanashi) are compared between them in terms of the temperature predicted for each case study of Tab. 3, under a wide range of input speed and input torque.

Figure 10 presents the temperature prediction for the three case studies, using the three methods, as function of the input speed. The results for Takanashi's method, in which the

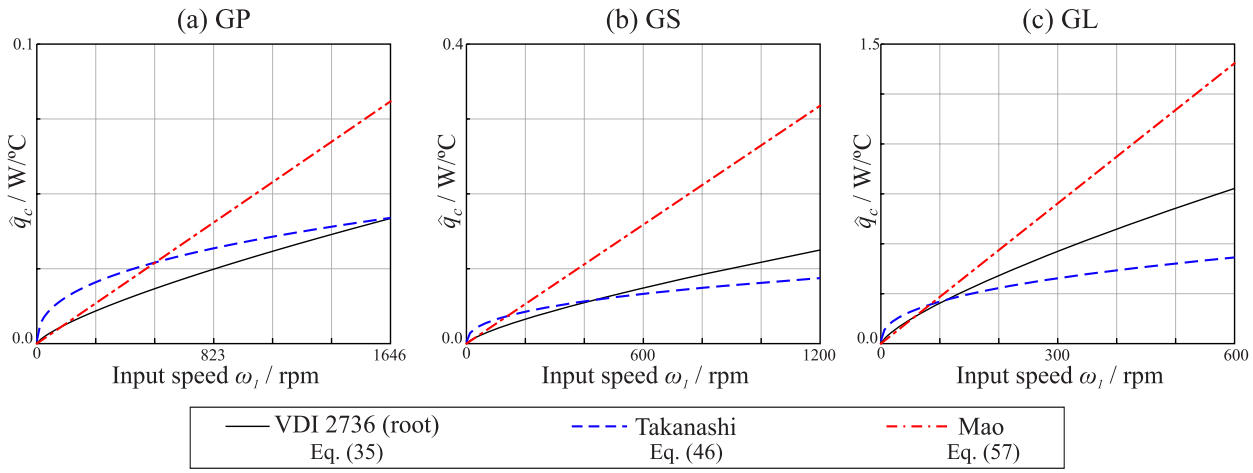

Figure 9: Influence of input speed on heat convection

hysteresis effect is neglected ($E_{h,th1} = 0$), are also displayed in Fig. 10. The figures also show results obtained from experiments [27, 37, 72], which are used as a reference for the evaluation of the selected methods. The results for case study GS include error bars, which are not available for remaining case studies.

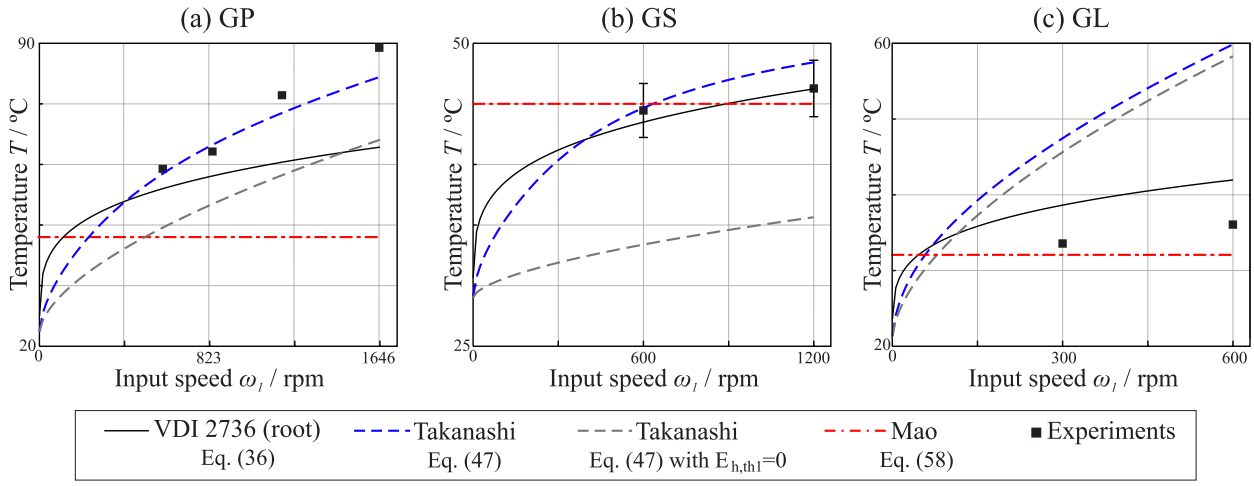

Figure 10: Influence of input speed on temperature at nominal input torque

Both VDI 2736 and Takanashi methods exhibit a non-linear relation between the angular speed and the temperature. In contrast, Mao's method is independent of the angular speed, and this can produce inaccuracies in those cases where angular speed is small [73]. While all the methods can accurately predict the operating temperature for the case study GS, for the case studies GL and GM they tend to diverge: Takanashi is closer to the experiments for GP case study, whereas Mao and VDI 2736 are closer to the experiments for GL case study.

Figure 11 presents the temperature prediction for the three case studies, using the three

methods, as function of the input torque. The results for Takanashi's method neglecting the effect of hysteresis are also displayed in the figure. The figures also show results obtained from experiments [27, 37, 72], which are used as a reference for the evaluation of the selected methods. The results for case study GS include error bars, which are not available for the remaining case studies.

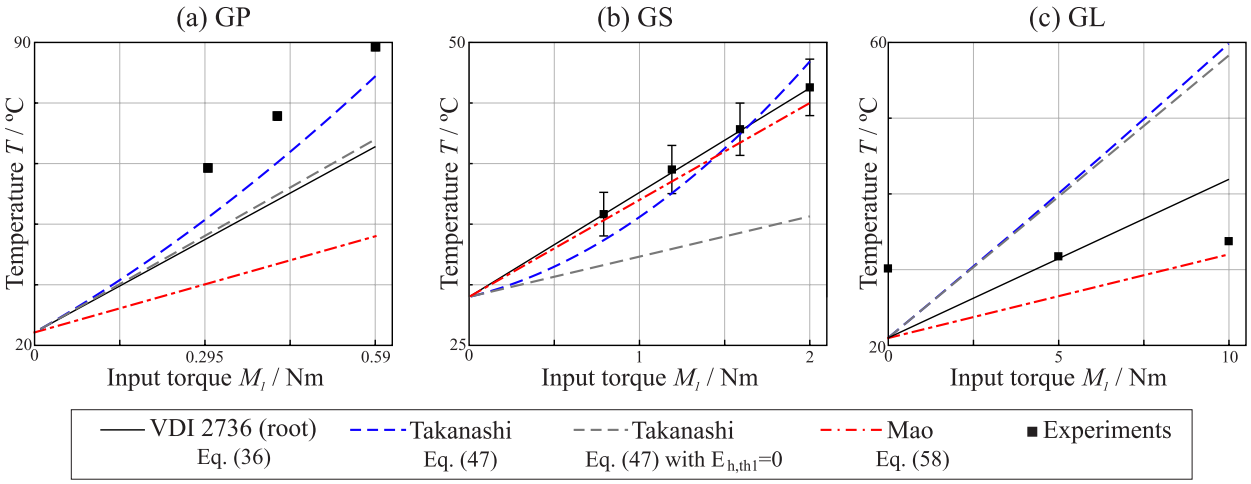

Figure 11: Influence of input torque on temperature at nominal input speed

All the methods present a linear dependency between temperature and torque, except for Takanashi's one, where a non-linear relation between the input torque and the temperature is obtained due to the consideration of hysteresis. Of course, the observed linear relation is only true if a constant coefficient of friction is considered with an increasing torque. Here, Takanashi presents the lowest deviation for case study GP, and VDI 2736 fits better for GS and GL. For the case study GS, all the methods perform relatively well.

Figure 11 also reveals the role that hysteresis plays in Takanashi's method. As expected from the previous discussion, hysteresis has the largest impact in case study GS, and the lowest impact in GL. In all the studied cases, it is observed that the increment of temperature due to hysteretic heat increases, as does the angular speed and the input torque. Moreover, the predominant effect of hysteretic heat in case study GS (Fig 11b) emphasizes the non-linear relation between temperature rise and input torque.

As a final remark, it can be said that the performance of the methods depends mostly on the selected coefficient of friction and heat transfer coefficient. In Fig. 11, the slope of the curves is ruled by the selected coefficient of friction and the heat transfer coefficient. In Fig 10, the behaviour of the curve is dictated by the selected Reynolds number when applying Newton's law of cooling, and the magnitude of the curve by the selected coefficient of friction and heat transfer coefficient.

10. Conclusions

In this work, analytical methods to predict the operating temperature of polymer gears are analysed and compared (VDI 2736, Takanashi and Mao methods). The temperature

of the gears is calculated based on the first law of thermodynamics by establishing an equilibrium between the heat generated during the meshing of the gears (by sliding friction and hysteresis of the material) and the heat dissipated from the gears by convection. Thus, each one of these methods is constituted by a heat generation model, and a heat dissipation model. The similarities and the differences between the heat generation and heat dissipation models affect the temperature results obtained from each one of the methods.

The analytical methods have been used to predict the operating temperature of three representative case studies, and the obtained results have been compared to experimental results, which has allowed us to draw the following conclusions:

1. Heat generated by sliding friction is considered in all the methods. For such a purpose, they use an approach based on the observation of the gear tooth contact through the line of action, considering a constant coefficient of friction and a stepped load sharing distribution. Compared to the theoretical solution, it can be said that Takanashi heat generation model is the most accurate one, followed by VDI 2736 and Mao model. The main difference between the models consists in the way in the heat partition factor calculation. Also, it is important to point out that Mao's heat generation model can only be successfully applied to gear transmissions in which the pinion and the wheel have the same geometry and the same material, and a transverse contact ratio of $\epsilon_\alpha = 1.5$.
2. Heat generated by hysteresis is only considered by Takanashi's method. Takanashi's method uses a Kelvin-Voigt model to determine the heat generated by hysteresis, and it has been verified that hysteretic heat can be neglected in those cases where the coefficient of friction is large enough. However, when the coefficient of friction is small, the hysteretic heat has a predominant effect over the frictional heat and, as a consequence, it should not be neglected.
3. In VDI 2736 and Takanashi methods, heat dissipated by convection is calculated using a model based on the Newton's law of cooling. To set up this model, it is required to conduct experiments to calculate the parameters that rule the behaviour of the heat transfer coefficient and the size of the convective area, which are critical parameters in order to obtain accurate temperature results. In Mao's method, heat dissipated by convection is calculated by approaching the gear transmission to a gear pump, which has the advantage of not requiring experiments to tune up the model. However, its applicability is limited to gear transmissions where both pinion and wheel have the same geometry, and it is only suitable for high input speeds.
4. Comparing the obtained results with experimental results, it is observed that Mao's method presents limited capabilities to predict the operating temperature of the gears. Between Takanashi and VDI 2736 methods it is not clear which one performed better among the case studies, as each one of them performed differently depending on the operating conditions.

Regardless of the final accuracy of the studied analytical methods, they have proven useful to understand the thermal behaviour of polymer gear transmissions. In order to improve

the accuracy of the results, further work must be done to include an accurate load sharing function and a time varying coefficient of friction in the heat generation model. In this line, the consideration of the temperature dependency of the tribological and material properties of the gears could also help increasing the degree of realism of the results. Regarding the heat dissipation model, further investigations should be made to improve the accuracy of the heat transfer coefficients.

Acknowledgments

The authors express their deep gratitude to Dr. Pedro M.T. Marques and MSc James Hooton for the analysis and suggestions for the manuscript.

Victor Roda-Casanova express his gratitude to the Universitat Jaume I for the financial support of research project ref. UJI-A2019-024.

Carlos M. C. G. Fernandes is grateful for the funding through LAETA in the framework of project UID/50022/2020.

References

[1] M. Kalin, A. Kupec, The dominant effect of temperature on the fatigue behaviour of polymer gears, Wear 376-377 (2017) 1339–1346. doi:10.1016/j.wear.2017.02.003.

[2] F. E. Kennedy, Frictional heating and contact temperatures, in: B. Bhushan (Ed.), Modern Tribology Handbook, CRC Press, Boca Raton, 2000, Ch. 6.

[3] H. Blok, The flash temperature concept, Wear 6 (1963) 483–494.

[4] B. Černe, M. Petkovšek, J. Duhovnik, J. Tavčar, Thermo-mechanical modeling of polymer spur gears with experimental validation using high-speed infrared thermography, Mechanism and Machine Theory 146 (4 2020). doi:10.1016/j.mechmachtheory.2019.103734.

[5] VDI-2736 Blatt 2: Thermoplastic gear wheels - Cylindrical gears - Calculation of the load-carrying capacity, Standard, Verein Deutscher Ingenieure, Dusseldorf, DE (2013).

[6] N. Anifantis, A. Dimarogonas, Flash and bulk temperatures of gear teeth due to friction, Mechanism and Machine Theory 28 (1993) 159–164.

[7] A. J. Housz, Scuffing as a factor in the design of nylon gears, Wear 10 (2) (1967) 118–126. doi:10.1016/0043-1648(67)90083-X.

[8] K. Mao, A numerical method for polymer composite gear flash temperature prediction, Wear 262 (2007) 1321–1329. doi:10.1016/j.wear.2007.01.008.

[9] N. P. Raghuraman, A calculation procedure to account for tolerances, transient temperature and humidity in the load distribution analysis of plastic and metal gears, Master's thesis, Graduate School of The Ohio State University, The Ohio State University (2013).

[10] B. Černe, J. Duhovnik, J. Tavčar, Semi-analytical flash temperature model for thermoplastic polymer spur gears with consideration of linear thermo-mechanical material characteristics, Journal of Computational Design and Engineering 6 (4) (2019) 617–628. doi:10.1016/j.jcde.2019.03.001.

[11] C. M. Fernandes, D. M. Rocha, R. C. Martins, L. Magalhães, J. H. Seabra, Finite element method model to predict bulk and flash temperatures on polymer gears, Tribology International 120 (2018) 255–268. doi:10.1016/J.TRIBOINT.2017.12.027.

[12] C. M. Fernandes, D. M. Rocha, R. C. Martins, L. Magalhaes, J. H. Seabra, Hybrid polymer gear concepts to improve thermal behavior, Journal of Tribology 141 (3 2019). doi:10.1115/1.4041461.

[13] V. Roda-Casanova, F. Sanchez-Marin, A. Porras-Vazquez, A fast finite element based methodology to predict the temperature field in a thermoplastic spur gear drive, in: Proceedings of the ASME Design Engineering Technical Conference, Vol. 10, 2017.

[14] V. Roda-Casanova, F. Sanchez-Marin, A 2D finite element based approach to predict the temperature field in polymer spur gear transmissions, Mechanism and Machine Theory 133 (2019) 195–210. doi:10.1016/j.mechmachtheory.2018.11.019.
[15] V. Roda-Casanova, I. Gonzalez-Perez, Investigation of the effect of contact pattern design on the mechanical and thermal behaviors of plastic-steel helical gear drives, Mechanism and Machine Theory 164 (10 2021). doi:10.1016/j.mechmachtheory.2021.104401.
[16] D. Miler, M. Hoić, Optimisation of cylindrical gear pairs: A review, Mechanism and Machine Theory 156 (2 2021). doi:10.1016/j.mechmachtheory.2020.104156.
[17] J. Tavčar, B. Cerne, J. Duhovnik, D. Zorko, A multicriteria function for polymer gear design optimization, Journal of Computational Design and Engineering 8 (2021) 581–599. doi:10.1093/jcde/qwaa097.
[18] T. Tobe, M. Kato, A study on flash temperatures on the spur gear teeth, Journal of Manufacturing Science and Engineering 96 (1974) 78–84. doi:https://doi.org/10.1115/1.3438333.
[19] K. Mao, The performance of dry running non-metallic gears, Ph.D. thesis, School of Manufacturing and Mechanical Engineering, The University of Birmingham (1993).
[20] R. Gauvin, P. Girard, H. Yelle, Maximum surface temperature of the thermoplastic gear in a non-lubricated plasticsteel gear pair, Gear Technology (1984).
[21] Engineering Sciences Data Unit, Design of parallel axis straight spur and helical non-metallic gears-Choice of material and load capacity., UK, 1977.
[22] H. Hachmann, E. Strickle, Polyamide als zahnradwerkstoffe, Konstruktion 18 (3) (1966) 81–94.
[23] BS 6168:1987 - Specification for non-metallic spur gears, Standard, British Standards Institution, London, UK (1987).
[24] D. Miler, M. Hoić, S. Škec, D. Žeželj, Optimisation of polymer spur gear pairs with experimental validation, Structural and Multidisciplinary Optimization 62 (2020) 3271–3285. doi:10.1007/s00158-020-02686-1.
[25] D. Zorko, S. Kulovec, J. Duhovnik, J. Tavčar, Durability and design parameters of a steel/peek gear pair, Mechanism and Machine Theory 140 (2019) 825–846. doi:10.1016/j.mechmachtheory.2019.07.001.
[26] D. Zorko, I. Demšar, J. Tavčar, An investigation on the potential of bio-based polymers for use in polymer gear transmissions, Polymer Testing 93 (1 2021). doi:10.1016/j.polymertesting.2020.106994.
[27] A. Pogacnik, J. Tavcar, Accelerated testing method for polymer gears. Review of gear body temperature calculation according to VDI 2736, in: VDI Gear Conference 2015, 2015.
[28] P. Faatz, G. W. Ehrenstein, Temperature calculation of plastic gears, in: ANTEC 2000, 2000, pp. 3–7.
[29] S. Takanashi, A. Shoji, Uber den temperaturanstieg von zahnen von kunststoffzahnradern (1. Bericht): Durch das eingreifen von kunststoffzahnradern erzeugte warmemenge, Science reports of the Research Institutes, Tohoku University. Ser. A, Physics, chemistry and metallurgy 28 (1979) 93–102.
[30] A. S. S. Takanashi, Uber den temperaturanstieg von zahnen von kunststoffzahnradern (2. Bericht): Uber die gleichgewichtstemperatur von zahnen von kunststoffzahnrader, Science reports of the Research Institutes, Tohoku University. Ser. A, Physics, chemistry and metallurgy 28 (1979) 103–115.
[31] S. Takanashi, A. Shoji, On the temperature rise in the teeth of plastic gears, in: International Power Transmission & Gearing Conference, San Francisco, 1980.
[32] S. Takanashi, A. Shoji, On the equilibrium temperature in the teeth of operating plastic gears, Bulleting Yamagata University 18 (1) (1984) 11–24.
[33] G. Erhard, Designing with Plastics, Carl Hanser Verlag GmbH & Company KG, Munich, 2006.
[34] K. Terashima, N. Tsukamoto, N. Nishida, J. Shi, Development of plastic gears for power transmission, Bulletin of JSME 29 (1986).
[35] C. M. Illenberger, T. Tobie, K. Stahl, Operating behavior and performance of oil-lubricated plastic gears, Forschung im Ingenieurwesen/Engineering Research (2021). doi:10.1007/s10010-021-00513-7.
[36] C. Hooke, K. Mao, D. Walton, A. Breeds, S. Kukureka, Measurement and prediction of the surface temperature in polymer gears and its relationship to gear wear, Journal of Tribology 115 (1) (1993) 119–124. doi:10.1115/1.2920964.
[37] P. K. Singh, Siddhartha, A. K. Singh, An investigation on the thermal and wear behavior of polymer based spur gears, Tribology International 118 (2018) 264–272. doi:10.1016/j.triboint.2017.10.007.

[38] D. Koffi, R. Gauvin, H. Yelle, Heat generation in thermoplastic spur gears, Journal of Mechanisms, Transmissions and Automation in Design 107 (1985) 31–36. doi:https://doi.org/10.1115/1.3258688.
[39] N. Doll, Modeling thermomechanical behavior of polymer gears, Master's thesis, Department of Mechanical Engineering, University of Wisconsin-Madison (2015).
[40] Y. Çengel, Heat Transfer: A Practical Approach, McGraw-Hill, 2003.
[41] ISO 21771:2007 Gears - Cylindrical involute gears and gear pairs — Concepts and geometry, Standard, International Organization for Standardization, Geneva, Switzerland (2007).
[42] B. E. Gurskii, A. Chichinadze, Frictional heat problem and its evolution. part 1. blok model and its improvement, Journal of Friction and Wear 28 (2007) 316–329. doi:10.3103/S1068366607030130.
[43] E. Buckingham, Analytical mechanics of gears, Dover Books for Engineers, McGraw-Hill Book Co., 1949.
[44] Y. A. Misharin, Influence of the friction condition on the magnitude of the friction coefficient in the case of rollers with sliding, Proceedings International Conference on Gearing, Institute Mechanical Engineers (1958).
[45] Y. Drozdov, Y. Gavrikov, Friction and scoring under the conditions of simultaneous rolling and sliding of bodies, Wear 11 (4) (1968) 291 – 302. doi:10.1016/0043-1648(68)90177-4.
[46] L. Schlenk, Unterscuchungen zur Fresstragfähigkeit von Grozahnrädern, Ph.D. thesis, Dissertation TU München (1994).
[47] X. Hai, Development of a generalized mechanical efficiency prediction methodology for gear pairs, Ph.D. thesis, The Ohio State University (2005).
[48] C. M. Fernandes, R. C. Martins, J. H. Seabra, Coefficient of friction equation for gears based on a modified Hersey parameter, Tribology International 101 (2016) 204–217. doi:10.1016/j.triboint.2016.03.028.
[49] S. Takanashi, A. Shoji, Measurement of the Coefficient of Kinetic Friction of Plastic Materials used for Gears, Journal of the Japan Society of Precision Engineering 47 (8) (1981) 944–948. doi:10.2493/jjspe1933.47.944.
[50] D. Miler, M. Hoić, Z. Domitran, D. Žeželj, Prediction of friction coefficient in dry-lubricated polyoxymethylene spur gear pairs, Mechanism and Machine Theory 138 (2019) 205–222. doi:10.1016/j.mechmachtheory.2019.03.040.
[51] Y. Chen, Y. Lin, A calculation method for friction coefficient and meshing efficiency of plastic line gear pair under dry friction conditions, Friction 9 (2021) 1420–1435. doi:10.1007/s40544-020-0424-x.
[52] R. Keresztes, L. Zsidai, G. Kalácska, M. Andó, R. Lefánti, Friction of Polymer/Steel Gear Pairs, Mechanical Engineering Letters 2 (2009) 1–11.
[53] A. J. Wimmer, Lastverluste von stirnradverzahnungen, Ph.D. thesis, Fakultät für Maschinenwesen der Technischen Universität München (2006).
[54] D. Walton, A. A. Tessema, C. J. Hooke, J. M. Shippen, Load sharing in metallic and non-metallic gears, Proceedings of the Institution of Mechanical Engineers, Part C: Journal of Mechanical Engineering Science 208 (2) (1994) 81–87.
[55] H. Yelle, D. Burns, Calculation of Contact Ratios for Plastic/Plastic or Plastic/Steel Spur Gear Pairs, Journal of Mechanical Design 103 (2) (1981).
[56] M. Karimpour, K. D. Dearn, D. Walton, A kinematic analysis of meshing polymer gear teeth, Proceedings of the Institution of Mechanical Engineers, Part L: Journal of Materials: Design and Applications 224 (2010) 101–115. doi:10.1243/14644207JMDA315.
[57] P. Langlois, Tooth contact analysis-off line of action contact and polymer gears, Gear Technology (2017).
[58] A. Singh, D. R. Houser, Analysis of off-line of action contact at the tips of gear teeth, SAE Transactions 103 (1994) 196–203.
[59] H. Ohlendorf, Verlustleistung und Erwärmung von Stirnrädern, Ph.D. thesis, Dissertation TU München (1958).
[60] G. Niemann, H. Winter, Maschinenelemente: Band 2: Getriebe allgemein, Zahnradgetriebe - Grundlagen, Stirnradgetriebe, Maschinenelemente /Gustav Niemann, Springer, 1989.
[61] C. M. C. G. Fernandes, P. M. T. Marques, R. C. Martins, J. H. O. Seabra, Influence of gear loss factor

on the power loss prediction, Mechanical Sciences 6 (2) (2015) 81–88. doi:10.5194/ms-6-81-2015.
[62] L. G. lxaru, G. V. Berghe, Runge-Kutta solvers for ordinary differential equations, in: M. Hazewinkel (Ed.), Exponential Fitting, Vol. 568, Springer Science, 2004, pp. 223–304.
[63] G. Niemann, Maschinenelemente. Bd.2, Springer-Verlag, 1960.
[64] DIN-EN 60034 Rotating electrical machines, Standard, Deutsches Institut für Normung, Berlin, DE (2010).
[65] S. Timoshenko, R. Baud, Strength of gear teeth is greatly affected by flllet radius, Automotive Industries 55 (1926) 138–142.
[66] R. Caldwell, Load sharing and elastic deformation in a gear mesh, Ph.D. thesis, Department of Mechanical Engineering, University of Akron (1986).
[67] C. Weber, K. Banaschek, Formänderung und Profilrücknahme bei Gerad-und Schrägverzahnten Antriebstechnik, F. Vieweg und Sohn, 1953.
[68] A. F. D. Rincon, F. Viadero, M. Iglesias, P. García, A. De-Juan, R. Sancibrian, A model for the study of meshing stiffness in spur gear transmissions, Mechanism and Machine Theory 61 (2013) 30–58. doi:10.1016/j.mechmachtheory.2012.10.008.
[69] J. D. Marafona, P. M. Marques, R. C. Martins, J. H. Seabra, Mesh stiffness models for cylindrical gears: A detailed review, Mechanism and Machine Theory 166 (12 2021). doi:10.1016/j.mechmachtheory.2021.104472.
[70] K. Mao, W. Li, C. J. Hooke, D. Walton, Friction and wear behaviour of acetal and nylon gears, Wear 267 (1-4) (2009) 639–645. doi:10.1016/j.wear.2008.10.005.
[71] K. Mao, P. Langlois, Z. Hu, K. Alharbi, X. Xu, M. Milson, W. Li, C. Hooke, D. Chetwynd, The wear and thermal mechanical contact behaviour of machine cut polymer gears, Wear 332-333 (2015) 822–826, 20th International Conference on Wear of Materials. doi:https://doi.org/10.1016/j.wear.2015.01.084.
[72] E. Letzelter, M. Guingand, J. P. D. Vaujany, P. Schlosser, A new experimental approach for measuring thermal behaviour in the case of nylon 6/6 cylindrical gears, Polymer Testing 29 (8) (2010) 1041–1051. doi:10.1016/j.polymertesting.2010.09.002.
[73] Z. Hu, An investigation into the wear and thermal-mechanical performance of polyacetal gears, Ph.D. thesis, School of Engineering, University of Warwick (2017).